Outer Valence Ionic States of $Cr(CO)_6$ and $(\eta^5\text{-}C_5H_5)Co(CO)_2$ Observed by Two-Dimensional Penning Ionization Electron Spectroscopy†

Naoki Kishimoto‡ and Koichi Ohno*,‡,§

Department of Chemistry, Graduate School of Science, Tohoku University, Aramaki, Aoba-ku, Sendai 980-8578, Japan, and Toyota Physics and Chemical Research Institute, Nagakute, Aichi 480-1192, Japan

Received: May 1, 2009; Revised Manuscript Received: July 30, 2009

Outer valence ionic states of $Cr(CO)_6$ and $(\eta^5\text{-}C_5H_5)Co(CO)_2$ were investigated by means of Penning ionization electron spectroscopy (PIES) upon collision with metastable $He^*(2^3S)$ excited atoms as well as high-level ab initio molecular orbital calculations taking electron correlation effects into consideration. By the 2D measurement combining the collision-energy-resolved technique of the metastable atomic beam and electron spectroscopy, ionic-state-resolved measurement of collision energy dependence of partial ionization cross sections (CEDPICS) was carried out. Because partial Penning ionization cross sections can be connected to the spatial extent of corresponding molecular orbitals (MOs) outside the boundary surface of colliding He* atoms, different slopes of CEDPICS were related to anisotropic interaction around the MO region. The observed CEDPICS and PIES band intensity were consistent with the order of calculated ionic states.

I. Introduction

To investigate the electronic structure of coordination compounds, electron spectroscopy methods and theoretical calculations of ionization energies have been utilized. For example, the investigation of the observed ultraviolet photoelectron spectrum (UPS) of ferrocene[1−3] was carried out by theoretical calculations of ionic states by post Hartree−Fock methods including electron correlation effects.[4,5] It should be noted that the ionization energy order for ionization from 3d orbitals of Fe is considerably different from that suggested by an SCF molecular orbital (MO) of ab initio Hartree−Fock calculation (Koopmans' theory), which is due to the importance of strong electron correlation effects and the break down of the one-to-one relationship between an orbital and an ionic state. A Green's functional method including electron correlation effects (ADC(3)) suggested many satellite bands of ferrocene in ionization energy larger than 10 eV.[4] The configuration interaction (CI) calculation by the SAC/SAC−CI theory indicated that the lowest two ionic states have significant components of shakeup configurations.[5]

Another measurement of ejected electrons for coordination compounds is Penning ionization electron spectroscopy (PIES) by collision with metastable atoms. By this method, orbital reactivity can be connected with spatial extent of MOs outside of the boundary surface of a colliding excited rare gas atom A* to a target molecule M[6]

$$A^* + M \rightarrow A + M^+ + e^- \qquad (1)$$

because the transition probability for the electron transfer from an occupied MO to the inner singly occupied orbital of A* mainly depends on the spatial overlap between the related orbitals. Reactivities of metal d orbitals of transition-metal complexes such as ferrocene[7−9] and other metallocenes[10] were found to be much smaller than those of ligand valence orbitals in the Penning ionization process, which means that metal d orbitals are shielded by ligands from the attack of the helium excited atoms. The shielding effect by ligands of metal complexes was also found for PIES of metal carbonyl compounds such as $Fe(CO)_5$[11] and $M(CO)_6$ (M = Cr, Mo, W).[12]

The change of orbital reactivity as a function of collision energy between metastable $He^*(2^3S)$ and metal coordination compounds can be observed by collision-energy-resolved technique of the metastable atomic beam. The 2D (collision-energy/electron-energy-resolved) Penning ionization electron spectroscopy (2D-PIES)[13] has enabled us to measure different collision energy dependences of partial ionization cross sections (CEDPICS) reflecting the anisotropic interaction between $He^*(2^3S)$ and a target molecule. In addition, different slopes of CEDPICS for each ionic state can be valuable for determining the assignment of the ionic state to related MOs. In this study, we have measured CEDPICS of $Cr(CO)_6$ and $(\eta^5\text{-}C_5H_5)Co(CO)_2$, and its different slope can be connected to ionization from metal d orbitals and ligand valence orbitals depending on the anisotropic interaction potential energy surface. Strong attractive interactions between targets and $He^*(2^3S)$ atoms were found around the oxygen atom of carbonyl groups in organic compounds such as HCHO and CH_2CHCHO,[14] whereas repulsive or weak attractive interaction was calculated for carbon monoxide (CO).[15] This difference in interaction may be related to the bond order of CO groups in organic molecules (double bond for C═O) or an inorganic molecule (triple bond for $C^-{\equiv}O^+$). In the case of ligand carbonyl groups, the bond order is thought to be between two and three because of the σ donation and π acceptance of electrons. For half-sandwich organometallic compounds such as $(\eta^6\text{-}C_6H_6)Cr(CO)_3$ and $(\eta^5\text{-}C_5H_5)Mn(CO)_3$,[16] attractive interaction with He* atoms was found around the π-orbital region of the hydrocarbon rings and the oxygen side of the ligand carbon monoxide group. Therefore, the interaction around the ligand carbonyl with $He^*(2^3S)$ atoms for $Cr(CO)_6$ and $(\eta^5\text{-}C_5H_5)Co(CO)_2$ is also interesting.

† Part of the "Vincenzo Aquilanti Festschrift".
* Corresponding author.
‡ Tohoku University.
§ Toyota Physics and Chemical Research Institute.

10.1021/jp9040524
Published on Web 08/31/2009

II. Methods

The experimental apparatus used in this study was reported in previous papers.[13] Beams of electronically excited metastable He*($2^{1,3}$S) atoms were produced by a nozzle discharge source with a tantalum hollow cathode.[17] The He*(2^1S) component was eliminated by a water-cooled helium discharge lamp (quench lamp), whereas He*(2^3S) metastable atoms (19.82 eV) were led to the collision cell in the reaction chamber. The background pressure in a reaction chamber was of the order of 10^{-7} Torr. We measured He I UPS by using the He I resonance photons (584 Å, 21.22 eV) produced by a discharge in pure helium gas. Sample molecules were purchased from a chemical company for $Cr(CO)_6$ (purchased from Aldrich) and (η^5-C_5H_5)$Co(CO)_2$ (purchased from Kanto Kagaku). We introduced the sample molecules to the main chamber without heating the sample tube, and the sample pressure in the main chamber was ca. 1×10^{-5} Torr. The kinetic energy of ejected electrons was measured by a hemispherical electrostatic-deflection-type analyzer using an electron collection angle of 90° relative to the incident He*(2^3S) or photon beam. The measurement of the full width at half-maximum (fwhm) of the $Ar^+(^2P_{3/2})$ peak in the He I UPS led to an estimate of 60 meV for the energy resolution of the electron energy analyzer. We determined the transmission efficiency curve of the electron energy analyzer by comparing our UPS data of some molecules with those by Gardner and Samson[18] and Kimura et al.[19]

In the experimental setup for the 2D Penning ionization electron measurement, the metastable atomic beam was modulated by a pseudorandom chopper[20] and then introduced to a reaction cell located at 504 mm downstream from the chopper disk. The measured Penning ionization spectra $I_e(E_e, t)$ were stored as a function of the electron kinetic energy (E_e) and time (t). The resolution of the analyzer was lowered to 250 meV to obtain higher counting rates of Penning electrons. The analysis of the time-dependent Penning ionization spectra by means of the Hadamard transformation and normalization by the velocity distribution of the He* beam can lead to a 2D mapping of the Penning ionization cross section as functions [σ (E_e, E_c)] of the electron energy (E_e) and collision energy (E_c). We determined the velocity distribution of the metastable He* beam by monitoring secondary electrons emitted from a stainless steel plate inserted in the reaction cell.

To obtain electron density contour maps of MOs, we performed SCF MO calculations. In the electron density contour maps, thick solid curves indicate the repulsive molecular surface approximated by atomic spheres of van der Waals radii.[21] The values of radius for the metal atoms were estimated from the half of metal−metal bond lengths plus an empirical value of 0.8 Å, which is roughly the difference between the van der Waals radii and the single-bond covalent radii for several main group elements.[21] The geometry of the sample was fully optimized by the density functional theory (DFT) with Becke's three-parameter exchange with the Lee, Yang, and Parr correlation functional (B3LYP)[22] with the 6-311G* basis set[23] for the metal atoms and cc-pVDZ basis set[24] for C, O, and H atoms. For the ionization potential energies, P3 propagator[25] and SAC/SAC−CI calculations were performed with the Gaussian 03 package program[26] with the same basis set used for the geometry optimization. In the SAC/SAC−CI calculation, the coefficient threshold for the ground-state configuration was lowered from 0.005 (default value) to 0.002, and the CISD solutions were used as the reference states. For the perturbation selection, "Level Two" was selected.

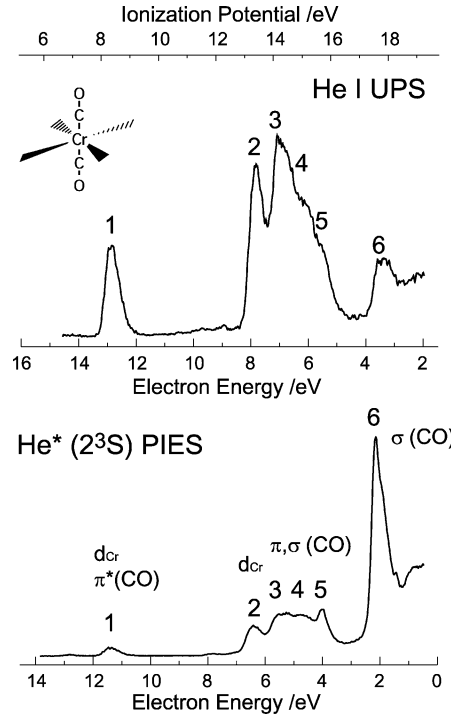

Figure 1. He I ultraviolet photoelectron spectrum (UPS) and He*(2^3S) Penning ionization electron spectrum (PIES) of $Cr(CO)_6$.

On the basis of the well-known resemblance between He*(2^3S) and Li(2^2S),[27] a Li(2^2S) atom in the ground state was utilized in place of a He*(2^3S) atom for potential energy surface calculations. This treatment enables us to avoid difficulties usually associated with ab initio MO calculations for highly excited states of a supermolecule consisting of a helium atom and an organometallic molecule. Interaction potentials between a Li(2^2S) atom and the sample molecules were calculated by DFT with the B3LYP functional and the Ahlrichs cc-pVDZ basis set[28] (metal atoms) and the 6-311+G* basis set (C, O, H, Li atoms).

III. Results

Figures 1 and 2 show He I UPS and He*(2^3S) PIES of $Cr(CO)_6$ and (η^5-C_5H_5)$Co(CO)_2$, respectively. Data of CEDPICS for $Cr(CO)_6$ and (η^5-C_5H_5)$Co(CO)_2$ are shown in Figures 3 and 4, respectively. The CEDPICS were obtained from the 2D-PIES $\sigma(E_c, E_e)$ within an appropriate range of E_e (typically fwhm of the band). Contour maps of electron densities for metal d and ligand valence MOs are also illustrated in Figures 3 and 4. The slope parameter (m) of CEDPICS listed in Tables 1 ($Cr(CO)_6$) and 2 ((η^5-C_5H_5)$Co(CO)_2$) was obtained by least-squares method. Calculated ionization potential (IP) energy values by Koopmans' theorem, P3, and SAC/SAC−CI[6] theory were also listed in the tables. The missing results by theoretical calculations in the tables are due to a convergence problem. The optimized structure of $Cr(CO)_6$ by DFT/B3LYP in this study is O_h symmetry, and the bond length was longer than experimental data[29] for crystalline $Cr(CO)_6$ within 0.01 Å. Regarding the optimized structure of (η^5-C_5H_5)$Co(CO)_2$, the C−Co−C bond angle ($\theta = 93.5°$) and the C−Co ($r_1 = 1.734$ Å) and C═O ($r_2 = 1.153$ Å) length of the carbonyl groups are somewhat different from experimental data by electron diffraction[30] or microwave[31] measurements ($\theta = 98°$, $r_1 = 1.679$ or 1.69 Å, $r_2 = 1.191$ Å). Interaction potential energy curves $V(R)$ as a function of the distance R for the model calculation of Li−M are shown in Figure 5.

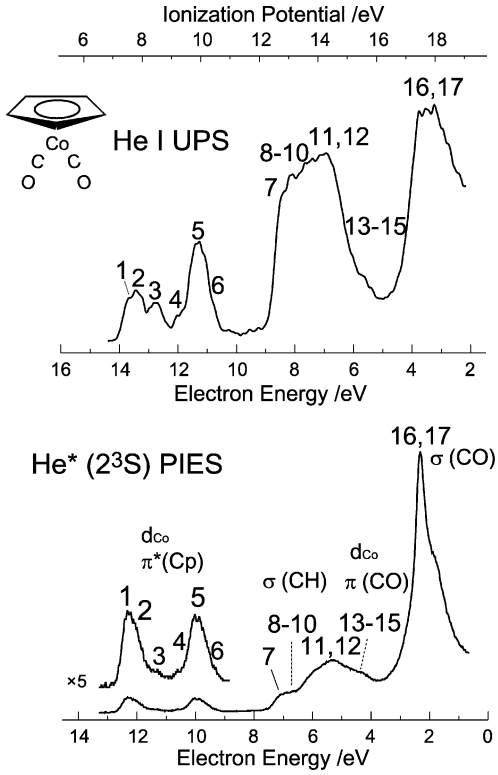

Figure 2. He I ultraviolet photoelectron spectrum (UPS) and He*(2^3S) Penning ionization electron spectrum (PIES) of $(\eta^5\text{-}C_5H_5)Co(CO)_2$.

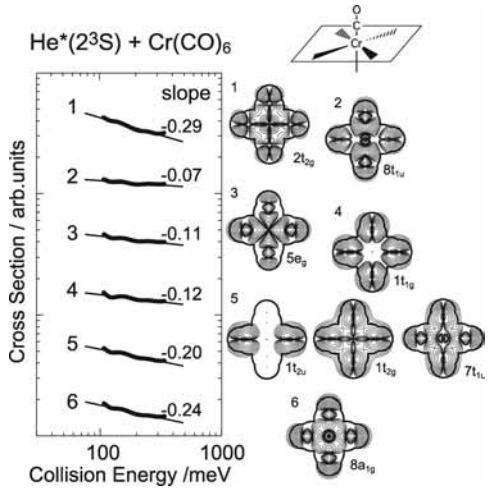

Figure 3. Collision energy dependence of partial ionization cross sections (CEDPICS) of $Cr(CO)_6$ by collision with He*(2^3S) atoms. Contour maps of electron densities for target MOs are also illustrated.

IV. Discussion

A. Ionization Electron Spectra of $Cr(CO)_6$ and $(\eta^5\text{-}C_5H_5)Co(CO)_2$. Observed bands in UPS and PIES are assigned to MOs based on the post SCF calculations in this study. Band 1 of $Cr(CO)_6$ and bands 1−6 of $(\eta^5\text{-}C_5H_5)Co(CO)_2$ were assigned to metal d and ligand π^* or π MOs. In electron exchange process[32] of Penning ionization, an electron of a target molecule transfers into the 1s orbital of He*(2^3S), and the excited electron is ejected to the continuum state simultaneously. Therefore, the transition probability mainly depends on spatial overlap between the target MO and the 1s orbital of He*, and the spatially extending distribution of an orbital results in large band intensity in PIES.[6,17] The small band intensity in PIES can be ascribed to the small overlap between the 1s hole of

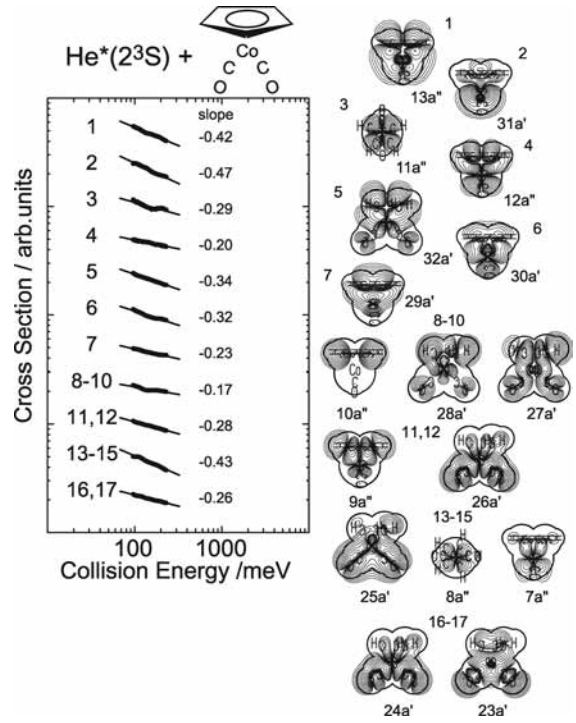

Figure 4. Collision energy dependence of partial ionization cross sections (CEDPICS) of $(\eta^5\text{-}C_5H_5)Co(CO)_2$ by collision with He*(2^3S) atoms. Contour maps of electron densities for target MOs are also illustrated.

He* atoms and MOs to be ionized around the metal atom and π-type orbital region. Band 2 of $Cr(CO)_6$ in PIES has a larger intensity than band 1, which is originated to the σ_{CO} component of the $8t_{1u}$ orbital rather than the π^*_{CO} component. For bands 1−6 of $(\eta^5\text{-}C_5H_5)Co(CO)_2$, the large spatial extent of 13a″ and 32a′ MOs resulted in a larger intensity of bands 1 and 5 than bands 2−4 and 6, and small band intensity of bands 3, 4, and 5 can be ascribed to the small spatial extent of 11a″, 12a″, and 30a′ MOs. These observed results are consistent with the order of ionic states calculated by SAC/SAC−CI theory in this study.

In the Penning ionization process, transition probability is zero at a nodal plane because the overlap between the 1s hole of He* and the target MO results in zero value at the nodal plane. For ionization from π_{CO} MOs of $Cr(CO)_6$, the transition can be limited because of the out-of-phase extent of π_{CO} MOs at the oxygen side of CO groups. This is the reason for the medium intensity of bands 4 and 5 for $Cr(CO)_6$ in PIES. Band 6 of $Cr(CO)_6$, which was assigned to σ_{CO} MOs by the SAC−CI calculation as well as the P3 calculation, showed remarkably enhanced intensity in PIES. This large intensity in PIES can be ascribed to the large electron density at the oxygen side of CO groups and in-phase extent of target MOs ($8a_{1g}$) for $Cr(CO)_6$. For the case of $(\eta^5\text{-}C_5H_5)Co(CO)_2$, the strong bands 16 and 17 were assigned to 24a′ and 23a′ MOs, which have σ_{CO} character, and the enhancement can be attributed to the large spatial distribution of the target MOs similarly to $Cr(CO)_6$. It should be noted that the in-phase extent of the π_{CO} MOs for $Cr(CO)_6$ ($1t_{2g}$) and $(\eta^5\text{-}C_5H_5)Co(CO)_2$ (26a′ and 25a′) was not directly connected to the enhancement of observed bands because the accessibility of He* to the root of ligand CO groups is limited.

Although Masuda et al. assigned[12] the enhanced band 6 in PIES of $Cr(CO)_6$ to three σ_{CO} MOs ($4e_g$, $6t_{1u}$, and $7a_{1g}$), which have lower orbital energy values than the $8a_{1g}$ MO, on the basis of the MS-Xα calculation,[33] the IP values for these MOs are 19.22−20.81 eV by the P3 calculation or 18.92−20.93 eV by

TABLE 1: Ionization Potentials (electronvolts) by He I UPS and Theoretical Calculations, Band Assignments, and Slope Parameter (*m*, See Text) of CEDPICS for $Cr(CO)_6$

band	IP	Koopmans[a]	P3[b]	SAC−CI[c]	*m*
1	8.35	9.43 ($2t_{2g}$, $d_{Cr} + \pi^*_{CO}$)		6.97 (0.67)	−0.29
2	13.40	16.22 ($8t_{1u}$, $d_{Cr} - \sigma_{CO} - \pi^*_{CO}$)	14.79 (0.89)	14.02 (0.66)	−0.07
3	14.15	16.72 ($5e_g$, $d_{Cr} + \sigma_{CO}$)	16.31(0.97)	14.63 (0.66)	−0.11
4	15.09	17.16 ($1t_{1g}$, π_{CO})	15.31 (0.82)	14.95 (0.60)	−0.12
5	15.53	17.36 ($1t_{2u}$, π_{CO})	15.49 (0.82)	15.18 (0.61)	−0.20
		17.95 ($1t_{2g}$, π_{CO})		15.47 (0.57)	
		17.99 ($7t_{1u}$, $\pi_{CO} + \sigma_{CO}$)	16.28 (0.85)	15.58 (0.61)	
6	17.64	19.71 ($8a_{1g}$, σ_{CO})	17.34 (0.85)	16.69 (0.25), 16.77 (0.36)	−0.24

[a] MO labels are shown in parentheses. [b] Pole strength values are shown in parentheses. [c] Intensities are shown in parentheses.

TABLE 2: Ionization Potentials (electronvolts) by He I UPS and Theoretical Calculations, Band Assignments, and Slope Parameter (*m*, See Text) of CEDPICS for $(\eta^5\text{-}C_5H_5)Co(CO)_2$

Band	IP	Koopmans[a]	P3[b]	SAC−CI[c]	*m*
1	7.59	7.92 (13a″, $d_{Co} - \pi^*_{Cp}$)		6.54 (0.70)	–0.42
2	7.94	11.41 (31a′, d_{Co})		6.59 (0.64)	–0.47
3	8.54	12.12 (11a″, d_{Co})		7.50 (0.64)	–0.29
4	9.35	13.56 (30a′, $d_{Co} - \pi_{Cp}$)		8.92 (0.66)	–0.20
5	10.00	9.31 (32a′, $d_{Co} + \pi^*_{Cp}$)	9.79 (0.92)	8.99 (0.71)	–0.34
6	10.49	11.77 (12a″, $d_{Co} + \pi^*_{Cp}$)		9.00 (0.69)	–0.32
7	(13.0)	14.27 (29a′, $d_{Co} + \pi_{Cp}$)	13.55 (0.94)	12.42 (0.69)	–0.23
8–10	(13.3)	14.36 (10a″, σ_{CH})	13.26 (0.92)	12.76 (0.73)	–0.17
		14.46 (28a′, σ_{CH})		12.79 (0.74)	
		14.89 (27a′, σ_{CH})	13.48 (0.90)		
11,12	(14.4)	15.50 (9a″, σ_{CH})	14.45 (0.95)	13.76 (0.72)	–0.28
		16.54 (26a′, σ_{CO})	15.20 (0.86)		
13–15	(15.5)	17.23 (25a′, π_{CO})	15.70 (0.85)		–0.43
		17.29 (8a″, d_{Co})	15.92 (0.88)		
		17.45 (7a″, d_{Co})	16.17 (0.90)		
16,17	17.64	17.56 (24a′, σ_{CO})	16.86 (0.96)		–0.26
		18.80 (23a′, σ_{CO})	17.21 (0.94)		

[a] MO labels are shown in parentheses. [b] Pole strength values are shown in parentheses. [c] Intensities are shown in parentheses.

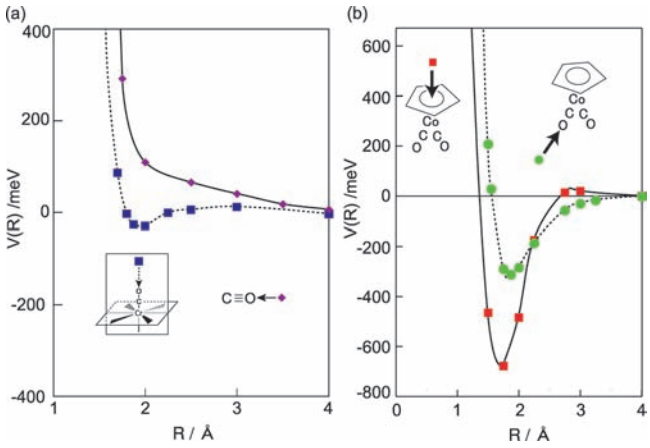

Figure 5. Interaction potential energy curves $V(R)$ for the model calculation between target molecules and Li atoms for (a) $Cr(CO)_6$ or CO and (b) $(\eta^5\text{-}C_5H_5)Co(CO)_2$. The distance R between the target and the Li atom is taken for (a) oxygen atom of $Cr(CO)_6$ or CO and (b) the center Co atom.

the SAC/SAC−CI theory in this study. The theoretical IPs are larger than the observed value (17.64 eV), and the three MOs may contribute to the signals in the low-energy region around 1 eV in PIES. When the assignment of band 6 in this study is correct, it follows that the enhancement of band 6 in PIES of $Cr(CO)_6$ compared with other σ_{CO} bands may be explained by another reason in addition to the large electron exterior distribution of the $8a_{1g}$ MO. It should be noted that σ_{CO} bands are remarkably enhanced in PIES for $Fe(CO)_5$,[11] $M(CO)_6$ (M = Cr, Mo, W),[12] and half-sandwiched complexes ($(\eta^6\text{-}C_6H_6)Cr(CO)_3$[16] and $(\eta^5\text{-}C_5H_5)Mn(CO)_3$,[16] and $(\eta^5\text{-}C_5H_5)Co(CO)_2$ in this study) regardless of the number of carbonyl groups. In a previous study, enhancement of inner valence carbon 2s (C_{2s}) bands was observed in PIES of $(CH_3)_4C$ and $(CH_3)_3CCl$ because of intermolecular excitation transfer ($He^*(2^3S) + M \rightarrow He + M^*$), followed by intramolecular Auger-like autoionization process involving electronic transition from an upper occupied MO to the inner C_{2s} hole.[34] We will discuss the possibility of this autoionization mechanism regarding the enhancement of σ_{CO} bands of $Cr(CO)_6$ and $(\eta^5\text{-}C_5H_5)Co(CO)_2$ in PIES in the next section.

A large low electron energy band (IP ≈ 18.5 eV) was observed for $(\eta^5\text{-}C_5H_5)Co(CO)_2$ in UPS. By the P3 method in this study, ionization energy values were calculated at 18.09 (21a′) and 18.23 eV (22a′) of $(\eta^5\text{-}C_5H_5)Co(CO)_2$. The in-phase extent of σ_{CH} (22a′ and 21a′) MOs may have relation with the large background signals at $E_e \approx 1$ eV in PIES.

B. Slope of Collision Energy Dependence of Partial Ionization Cross Sections. The negative slope of CEDPICS can be ascribed to attractive interaction between the target molecule and $He^*(2^3S)$ atoms. It is known that slower He* atoms can enter the reactive region more than the case of faster He* atoms because of the lower centrifugal barrier, which can lead to negative CEDPICS.[13−17] When the attractive part R^{-s} of the interaction potential is dominant (R is the distance between the target and the projectile), ionization cross section $\sigma(E_c)$ can be expressed[27] by

$$\sigma(E_c) \propto E_c^{-2/s} \qquad (2)$$

This formula was derived from the impact parameter for which orbiting occurs for atomic targets, and the slope of log $\sigma(E_c)$ versus log E_c plot can be connected to the function form ($m = -2/s$).

In the results of the model calculation, strongly attractive potential well was obtained for the model potential calculation (Figure 5) for the access of Li to the π_{Cp} and σ_{CO} orbital regions of $(\eta^5\text{-}C_5H_5)Co(CO)_2$. Although interaction between a target molecule and He* is large around carbonyl groups of $Cr(CO)_6$ rather than the repulsive case of CO,[15] the calculated attractive interaction around the oxygen atom was weak for $Cr(CO)_6$ in comparison with $(\eta^5\text{-}C_5H_5)Co(CO)_2$. These results are consistent with the observed negative slope of CEDPICS for band 1 ($d_{Co} - \pi^*_{Cp,}$ $m = -0.42$), band 2 ($d_{Co,}$ $m = -0.47$), band 5 ($d_{Co} + \pi^*_{Cp,}$ $m = -0.34$), and band 13 ($\pi_{CO,}$ $m = -0.43$) of $(\eta^5\text{-}C_5H_5)Co(CO)_2$ and band 1 ($d_{Cr} + \pi^*_{CO,}$ $m = -0.29$) and band 6 ($\sigma_{CO,}$ $m = -0.24$) of $Cr(CO)_6$.

Regardless of the different degree of attractive interactions, slope values of CEDPICS for the remarkably enhanced σ_{CO} bands are similar for $(\eta^5\text{-}C_5H_5)Co(CO)_2$ ($m = -0.26$) and $Cr(CO)_6$ ($m = -0.24$), which may be related to the Auger-like autoionization process mentioned in the previous section. The estimated energy values of inner $7a_{1g}$ MO of $Cr(CO)_6$ ($\varepsilon = -23.36$ eV) and 18a′ MO of $(\eta^5\text{-}C_5H_5)Co(CO)_2$ ($\varepsilon = -26.40$ eV), whose symmetries are the same as those of the enhanced bands, are near the 1s orbital of He* ($\varepsilon = -24.59$ eV) and suitable for the resonance followed by Auger-like autoionization. It should be noted that similar small CEDPICS ($m = -0.28$) were observed for the S_{3s} Auger-like autoionization process of CH_3SSCH_3,[35] and the resonance state may occur at long-range distance between M and He*(2^3S).

Overlapping bands 2−5 of $Cr(CO)_6$ originate from 5σ- or 1π-type MOs of CO. Observed negative CEDPICS mean that the attractive interaction region spreads all around the molecule, and the extent of the influence of the interaction from $m = -0.07$ (band 2) to -0.20 (band 5) can be different depending on the anisotropic distribution of MOs to be ionized. In the case of $(\eta^5\text{-}C_5H_5)Co(CO)_2$, repulsive interaction around the σ_{CH} orbital region resulted in the small negative slope of CEDPICS for bands 8−10 (σ_{CH}, $m = -0.17$). The observed large negative slope of CEDPICS for bands 13−15 ($m = -0.43$) can be attributed to the in-phase extent of π_{CO} MO (25a′), which is different from the case $1t_{2g}$ MO of $Cr(CO)_6$ (band 5, $m = -0.20$). In this study, we calculated natural charge (δ) for the oxygen atom of $(\eta^5\text{-}C_5H_5)Co(CO)_2$ and $Cr(CO)_6$ by the B3LYP method. The obtained δ values for $(\eta^5\text{-}C_5H_5)Co(CO)_2$ and $Cr(CO)_6$ are -0.46 and -0.43, respectively. This small difference between negative δ values is not dominant for the difference of interaction with He*. Interorbital interactions between the 2s orbital of He* and target MOs with larger MO energy level are more favorable, and the energy level of HOMO for $(\eta^5\text{-}C_5H_5)Co(CO)_2$ is higher than that of $Cr(CO)_6$ judged from the first IP value in UPS. In addition, the first IP of carbon monoxide is 14 eV, which is consistent with repulsive interaction with He* atoms.

V. Conclusions

Penning ionization of $Cr(CO)_6$ and $(\eta^5\text{-}C_5H_5)Co(CO)_2$ by collision with He*(2^3S) metastable atoms was observed with collision-energy-resolved 2D electron spectroscopy. CEDPICS for each ionic state indicate that strong attractive interaction around the cyclopentadienyl rings (Cp) resulted in negative slope of CEDPICS for ionization from valence π_{Cp} orbtials. A repulsive interaction was also found around the σ_{CH} bonds of the Cp ring.

Observed ionic states were assigned to MOs based on high-level ab initio MO calculations (SAC/SAC−CI and P3) taking electron correlation effects into consideration, which is consistent with the band intensity in PIES and the negative slope of CEDPICS. Although strong and weak attractive interactions were obtained around the oxygen side of carbonyl groups by the Li model calculations for $(\eta^5\text{-}C_5H_5)Co(CO)_2$ and $Cr(CO)_6$, respectively, similar negative slope values of CEDPICS were observed for the remarkably enhanced σ_{CO} bands of both sample molecules.

Acknowledgment. This research was supported by a Grant for Scientific Research from the Japan Society for the Promotion of Science. We thank Dr. Hideyasu Tanaka and Mr. Shimpei Fukuoka for valuable contribution to the experiment and calculations in this study.

References and Notes

(1) Rabalais, J. W.; Werme, L. O.; Bergmark, T.; Karlsson, L.; Hussain, M.; Siegbahn, K. *J. Chem. Phys.* **1972**, *57*, 1185.
(2) Evans, S.; Green, M. L. H.; Jewitt, B.; Orchard, A. F.; Pygall, C. F. *J. Chem. Soc., Faraday Trans. 2* **1972**, *68*, 1847.
(3) Cauletti, C.; Green, J. C.; Kelly, M. R.; Powell, P.; Tilberg, J. V.; Robbins, J.; Smart, J. *J. Electron Spectrosc. Relat. Phenom.* **1980**, *19*, 327.
(4) Ohno, M.; von Niessen, V.; Schüle, J. *Chem. Phys.* **1991**, *1*, 158.
(5) Ishimura, K.; Hada, M.; Nakatsuji, H. *J. Chem. Phys.* **2002**, *117*, 6533.
(6) Ohno, K.; Mutoh, H.; Harada, Y. *J. Am. Chem. Soc.* **1983**, *105*, 4555.
(7) Munakata, T.; Harada, Y.; Ohno, K.; Kuchitsu, K. *Chem. Phys. Lett.* **1981**, *84*, 6.
(8) Masuda, S.; Aoyama, M.; Harada, Y. *J. Am. Chem. Soc.* **1990**, *112*, 6445.
(9) Kishimoto, N.; Ohno, K. *J. Phys. Chem. A* **2009**, *113*, 521.
(10) Mutoh, H.; Masuda, S. *J. Chem. Soc., Dalton Trans.* **2002**, 1875.
(11) Harada, Y.; Ohno, K.; Mutoh, H. *J. Chem. Phys.* **1983**, *79*, 3251.
(12) Masuda, S.; Harada, Y. *J. Chem. Phys.* **1992**, *96*, 2469.
(13) Kishimoto, N.; Ohno, K. *Int. Rev. Phys. Chem.* **2007**, *26*, 93.
(14) Ohno, K.; Okamura, K.; Yamakado, H.; Hoshino, S.; Takami, T.; Yamauchi, M. *J. Phys. Chem.* **1995**, *99*, 14247.
(15) Maeda, S.; Yamazaki, M.; Kishimoto, N.; Ohno, K. *J. Chem. Phys.* **2004**, *120*, 781.
(16) Kishimoto, N.; Fukuoka, S.; Tanaka, H.; Ohno, K. *J. Electron Spectrosc. Relat. Phenom.* **2004**, *313*, 137–140.
(17) Ohno, K. *Bull. Chem. Soc. Jpn.* **2004**, *77*, 887.
(18) Gardner, J. L.; Samson, J. A. R. *J. Electron Spectrosc. Relat. Phenom.* **1976**, *8*, 469.
(19) Kimura, K.; Katsumata, S.; Achiba, Y.; Yamazaki, T.; Iwata, S. *Handbook of He I Photoelectron Spectra of Fundamental Organic Molecules*; Japan Scientific Societies Press: Tokyo, Japan, 1981.
(20) Kishimoto, N.; Aizawa, J.; Yamakado, H.; Ohno, K. *J. Phys. Chem. A* **1997**, *101*, 5038.
(21) Pauling, L. *The Nature of the Chemical Bond*; Cornell University: Ithaca, NY, 1960.
(22) Becke, A. D. *J. Chem. Phys.* **1993**, *7*, 5648.
(23) (a) Wachters, A. J. H. *J. Chem. Phys.* **1970**, *52*, 1033. (b) Hay, P. J. *J. Chem. Phys.* **1977**, *66*, 4377.
(24) Dunning, T. H., Jr. *J. Chem. Phys.* **1989**, *90*, 1007.
(25) Ortiz, J. V. *J. Chem. Phys.* **1996**, *104*, 7599.
(26) Frisch, M. J.; Trucks, G. W.; Schlegel, H. B.; Scuseria, G. E.; Robb, M. A.; Cheeseman, J. R.; Montgomery, J. A., Jr.; Vreven, T.; Kudin, K. N.; Burant, J. C.; Millam, J. M.; Iyengar, S. S.; Tomasi, J.; Barone, V.; Mennucci, B.; Cossi, M.; Scalmani, G.; Rega, N.; Petersson, G. A.; Nakatsuji, H.; Hada, M.; Ehara, M.; Toyota, K.; Fukuda, R.; Hasegawa, J.; Ishida, M.; Nakajima, T.; Honda, Y.; Kitao, O.; Nakai, H.; Klene, M.; Li, X.; Knox, J. E.; Hratchian, H. P.; Cross, J. B.; Bakken, V.; Adamo, C.; Jaramillo, J.; Gomperts, R.; Stratmann, R. E.; Yazyev, O.; Austin, A. J.; Cammi, R.; Pomelli, C.; Ochterski, J. W.; Ayala, P. Y.; Morokuma, K.; Voth, G. A.; Salvador, P.; Dannenberg, J. J.; Zakrzewski, V. G.; Dapprich, S.; Daniels, A. D.; Strain, M. C.; Farkas, O.; Malick, D. K.; Rabuck, A. D.; Raghavachari, K.; Foresman, J. B.; Ortiz, J. V.; Cui, Q.; Baboul, A. G.; Clifford, S.; Cioslowski, J.; Stefanov, B. B.; Liu, G.; Liashenko, A.; Piskorz, P.; Komaromi, I.; Martin, R. L.; Fox, D. J.; Keith, T.; Al-Laham, M. A.; Peng, C. Y.; Nanayakkara, A.; Challacombe, M.; Gill, P. M. W.; Johnson, B.; Chen, W.; Wong, M. W.; Gonzalez, C.; Pople, J. A. *Gaussian 03*, revision C.02; Gaussian, Inc.: Wallingford, CT, 2004.
(27) Niehaus, A. *Adv. Chem. Phys.* **1981**, *45*, 399.
(28) Schafer, A.; Horn, H.; Ahlrichs, R. *J. Chem. Phys.* **1992**, *97*, 2751.

(29) Rees, B.; Mitschler, A. *J. Am. Chem. Soc.* **1976**, *98*, 7872.

(30) Beagley, B.; Parrott, C. T.; Ulbrecht, V.; Young, G. G. *J. Mol. Struct.* **1979**, *52*, 47.

(31) Roehrig, M. A.; Chen, Q. Q.; Haubrich, S. T.; Kukolich, S. G. *Chem. Phys. Lett.* **1991**, *183*, 84.

(32) Hotop, H.; Niehaus, A. *Z. Phys.* **1969**, *228*, 68.

(33) Johnson, J. B.; Klemperer, W. G. *J. Am. Chem. Soc.* **1977**, *99*, 7132.

(34) Takami, T.; Mitsuke, K.; Ohno, K. *J. Chem. Phys.* **1991**, *95*, 918.

(35) Kishimoto, N.; Yokoi, R.; Yamakado, H.; Ohno, K. *J. Phys. Chem. A* **1997**, *101*, 3284.

JP9040524